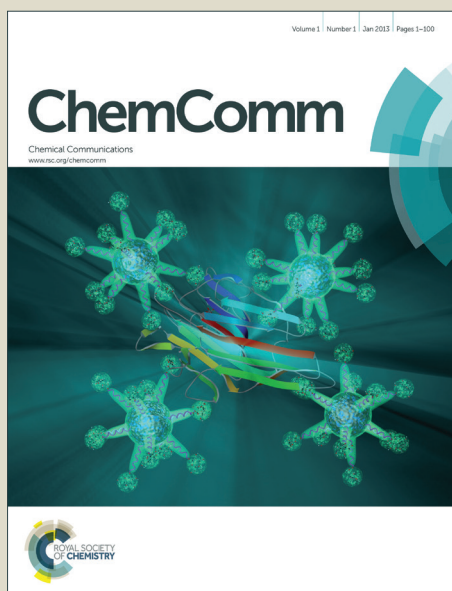


ChemComm

Accepted Manuscript



This article can be cited before page numbers have been issued, to do this please use: X. Zhan, J. Zhang, S. Tang, Y. Lin, M. Zhao, J. Yang, H. Zhang, Q. Peng, G. Yu and Z. Li, *Chem. Commun.*, 2015, DOI:



This is an *Accepted Manuscript*, which has been through the Royal Society of Chemistry peer review process and has been accepted for publication.

Accepted Manuscripts are published online shortly after acceptance, before technical editing, formatting and proof reading. Using this free service, authors can make their results available to the community, in citable form, before we publish the edited article. We will replace this *Accepted Manuscript* with the edited and formatted *Advance Article* as soon as it is available.

You can find more information about *Accepted Manuscripts* in the [Information for Authors](#).

Please note that technical editing may introduce minor changes to the text and/or graphics, which may alter content. The journal's standard [Terms & Conditions](#) and the [Ethical guidelines](#) still apply. In no event shall the Royal Society of Chemistry be held responsible for any errors or omissions in this *Accepted Manuscript* or any consequences arising from the use of any information it contains.

COMMUNICATION

Pyrene fused perylene diimides: synthesis, characterization and applications in organic field-effect transistors and optical limiting with high performance

Cite this: DOI: 10.1039/x0xx00000x

Received 00th January 2012,
Accepted 00th January 2012

DOI: 10.1039/x0xx00000x

www.rsc.org/

Xuejun Zhan,^a Ji Zhang,^b Sheng Tang,^a Yuxuan Lin,^a Min Zhao,^c Jie Yang,^a Haoli Zhang,^{*c} Qian Peng,^b Gui Yu,^{*b} and Zhen Li^{*a}

Three pyrene fused PDI derivatives have been obtained, in which totally different properties were observed when adopting different fusing type. For bilaterally benzannulation PDI, through spin-coating, bottom-contact OFET devices exhibited p-type mobility up to 1.13 cm² V⁻¹ s⁻¹, with an on/off ratio of 10⁸ in air.

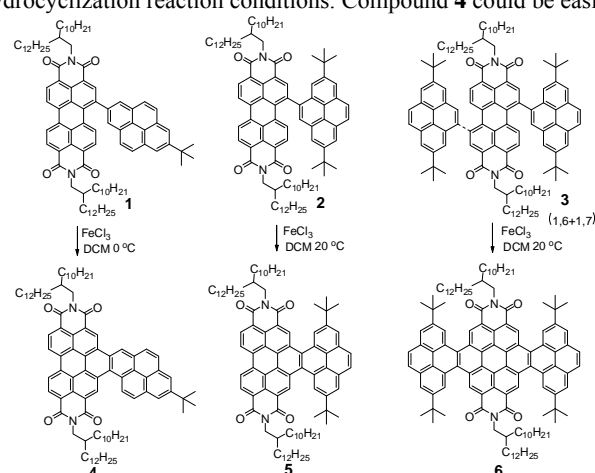
Perylene tetracarboxdiimide derivatives (PDIs) have gained considerable attention due to their special π -conjugation structure and opto-electronic properties,¹ in addition to their exclusive chemical, thermal and photochemical stability.² Many PDI-containing conjugated molecules and polymers exhibited exciting performance.³ For example, when utilized in organic transistors, as reported by Ichikawa et al.,⁴ the tridecyl-substituted PDI showed n-type mobility up to 2.1 cm² V⁻¹ s⁻¹, while an electron mobility of 1.24 cm² V⁻¹ s⁻¹ was realized for 2,2,3,3,4,4,4-heptafluorobutyl-substituted PDI by Würthner et al. (Chart S1).⁵ Meanwhile, when acting as electron acceptor in polymer solar cells instead of normal fullerenes, Nuckolls et al. achieved a high power convert efficiency of 6.1% by using a helical PDI dimer (Chart S2).⁶

Generally, there were two main approaches to design PDIs, an easy one is the functionalization at the main or bay positions of PDI, and another is the extension of the aromatic core of PDI, to yield fused PDIs. Although the latter one was much more difficult with synthetic challenge, their promising applications in different fields prompted scientists, with great efforts, to design various heterocycle-fused PDIs,⁷ with the adjusted electrical characteristics, including anthraquinone, pyridine, imidazole, pyrazole, triazole and even naphthalene tetracarboxdiimide (NDI) or PDI itself. Interestingly, on the other hand, as important synthetic precursors for polycyclic aromatic hydrocarbons (PAHs),⁸ a special model to understand the structure-property relationship⁹ of the unique graphene because of the structure similarity, fused PDIs were also required to be prepared with different but elaborately designed structures. Thanks to the great enthusiasm of scientists, some aromatic hydrocarbons fused PDIs were successfully obtained,¹⁰ with the anthracene fused PDI as the largest aromatic hydrocarbons fused PDI derivative up to date (Chart S3). However, the family of aromatic hydrocarbons fused PDIs was far from sufficient, mainly caused by the relatively bad

reactivity of larger hydrocarbon aromatic rings and the challenge to control structure specificity, especially for bilaterally extension.

To enrich the fused PDI family, and explore their structure-property relationship, in this communication, three core expanded PDI derivatives were synthesized, in which, pyrene,¹¹ an attractive unit with unique electronic and photophysical property, was utilized to fuse with the PDI core in different mode. To the best of our knowledge, this is the first time that pyrene fused PDI derivatives were designed and applied in organic electronics.

The synthetic route is depicted in Scheme 1, and the experimental details are provided in the ESI.† By utilizing the iridium-catalyzed reactions,¹² 2-Bpin-7-*tert*-butylpyrene and 4-Bpin-2,7-di-*tert*-butylpyrene were synthesized and then used to construct compounds **1**, **2** and **3** conveniently through the palladium (0)-catalyzed Suzuki cross coupling reaction, which were further cyclized to yield **4**, **5** and **6**, respectively, in the presence of ferric chloride. Notably, the K-region of pyrene aided to eliminate the possible isomers, when cyclization reaction occurred during the synthesis of bilaterally extension PDI derivative **6**, since **PDI-2Br** is a mixture of 1,6- and 1,7-substituted ones. Interestingly, there are some differences for the dehydrocyclization reaction conditions. Compound **4** could be easily



Scheme 1 Synthetic route of the pyrene fused PDI derivatives.

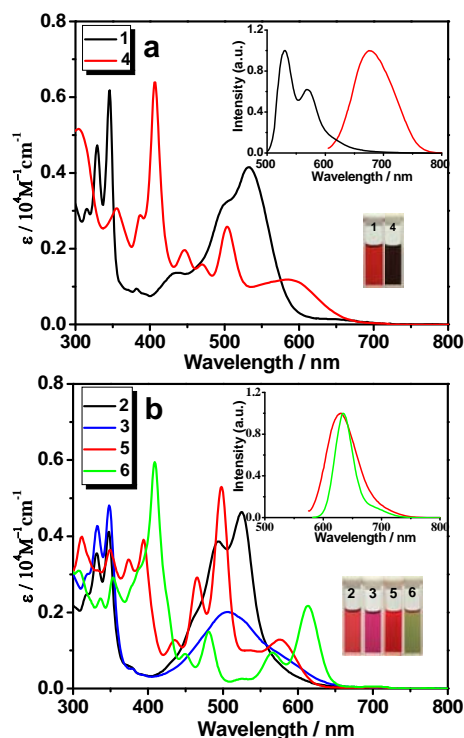


Fig. 1 UV-vis absorption and fluorescence emission (inset) spectra of **1**, **4** (a) and **2**, **3**, **5**, **6** (b) in dichloromethane. The inset pictures are photographs under sunlight.

gotten, when its precursor, compound **1**, reacted with 10 equivalent of ferric chloride at 0 °C for 30 min. But for **5**, adopting another fusing type, higher temperature (20 °C) and longer reaction time (70 min) were required, probably due to the different reactivity of the 1- and 5-positions of pyrene unit or/and the different distances between the dehydrogenation sites (Fig. S2).¹³ All of these compounds were easily purified by column chromatography on silica gel using petroleum ether-chloroform as eluent, and fully characterized by ¹H and ¹³C NMR, mass spectrometry, and elemental analysis, with the data presented in the ESI.

Thanks to the long branched alkyl chains, all the compounds have good solubility in common organic solvents, such as dichloromethane, chloroform and tetrahydrofuran (THF) et al.. Fig. 1 shows their absorption spectra in diluted dichloromethane (DCM) solutions. Compound **1** and **2**, with a donor-acceptor (D-A) structure, show similar absorptions, in which the bands around 350 and 500 nm can be respectively attributed to the absorption of pyrene and perylene bisimide unit. Dipyrrene substituted PDI (**3**) shows similar, however, broader absorption in the long wavelength region (400-650 nm) possibly derived from its D-A-D structure, similar to the UV-vis absorption of dianthracene substitution PDIs reported in literature.^{10b} After cyclization, absorptions of the pyrene units are red-shifted (about 50 nm), while the absorptions of perylene bisimide units are blue-shifted, as the results of the enlarged conjugation.¹¹ For **4** and **5**, due to the different fusing types, the typical shoulder bands caused by HOMO-LUMO transition¹⁰ appear at around 600 or 570 nm, respectively, which partially reflects the better electron delocalization of the fused type in **4**. For bilaterally extension **6**, the absorbance of perylene bisimide is relatively low, and two new peaks around 560 and 613 nm are observed. Theoretical calculation was also carried out by the TD-DFT method at the B3LYP/6-311G (d, p) level to investigate the electronic transitions (Fig. S3-S5, Table S1-S2). The electronic transition

analysis of compound **4** suggests that the band at 600 nm is caused by a transition from a pyrene-like HOMO to a PDI-like LUMO ($f = 0.13$), while the transition in compound **1** is weak ($f = 0.0052$).

The cyclization precursors **1**, **2** and **3**, show weak emission in DCM solutions, and their fluorescent quantum yields are estimated to be 2.89%, 0.13% and 0.24%, respectively. After cyclization, **4** emits at 676 nm weakly ($\Phi_F = 1.21\%$), while compounds **5** ($\Phi_F = 21.1\%$) and **6** ($\Phi_F = 20.2\%$) show increased emission intensities at 630 and 635 nm, respectively. Comparing **4** and **5** carefully, the different fused type induced a big difference of the emission wavelengths. In addition, through transient spectra (Fig. S3) for **1**, **2**, **3**, **4**, **5** and **6**, their fluorescence lifetimes were estimated to be 0.95, 0.48, 1.37, 5.05, 8.51 and 5.15 ns, respectively. All the fused compounds show increased lifetimes in comparison with their precursors.

Cyclic voltammetry (CV) measurements were carried out to investigate the electrochemical properties of these new PDI-based compounds. In their CV curves, all the compounds bear two one-electron reduction processes (Fig. S4). After cyclization, the first oxidation potential and the first reduction potential are both negatively shifted, indicating that they are easier to be oxidized but more difficult to be reduced. For **1**, **2**, **3**, **4**, **5** and **6**, their HOMO values are calculated to be -5.68, 5.64, -5.59, -5.54, -5.61 and -5.45 eV, respectively. Their corresponding LUMO energy levels are calculated to be -3.59, -3.57, -3.68, -3.68, -3.61 and -3.56 eV, respectively. The smaller band-gap of **4** (1.86 eV) than that of **5** (2.00 eV) further proved that the fused type in **4** can induce better conjugation. However, with the bilateral structure, the band-gap of **6** could be as low as 1.89 eV, owing to its enlarged planar π system.

To obtain some information at the molecular level, we have carried out Density Functional Theory (DFT) calculations (B3LYP/6-31G*) of these compounds to obtain the optimized structures and orbital distributions of HOMO and LUMO energy levels. As demonstrated in Fig. 2, the electron clouds of HOMO energy levels are all mainly located on the pyrene units, while the LUMOs are dominated by orbitals from perylene bisimides. While for **6**, because of the extended conjugation, the electron clouds of HOMO energy level are more delocalized. Theoretical calculated HOMO and LUMO energy levels and band-gaps are shown in Table S1. The predicted values of band-gaps for cyclization products **4**, **5**, **6** are calculated to be 2.22, 2.41, 2.32 eV, respectively, about 0.4 eV larger than their optical band-gaps.

The research of organic field-effect transistors (OFETs) is of great importance to the development of radio frequency identification (RFID) tags, flexible displays, electronic papers, sensors, and so forth.¹⁴ Even though lots of π -conjugated systems have been developed for OFETs, those with high mobility over $1.0 \text{ cm}^2 \text{ V}^{-1} \text{ s}^{-1}$ and easily to be solution-processed are still scarce.^{3c} Considering its large planar structure, special electronic property, and good solubility, the mobility of **6** was tested. OFETs were fabricated in a "bottom-contact" configuration. Before the deposition of organic semiconductors, source and drain electrodes made of gold were prepared on the SiO₂/Si substrates. The octyltrichlorosilane (OTS)

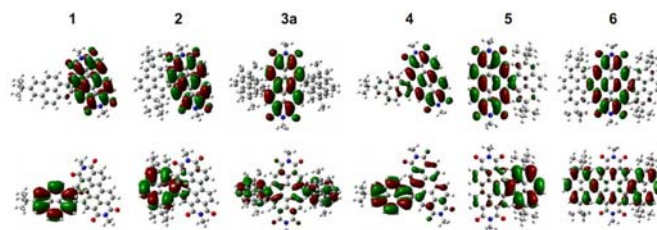


Fig. 2 Calculated molecular orbital amplitude plots of HOMO (down) and LUMO (up) levels of **1**, **2**, **3a**, **4**, **5** and **6**.

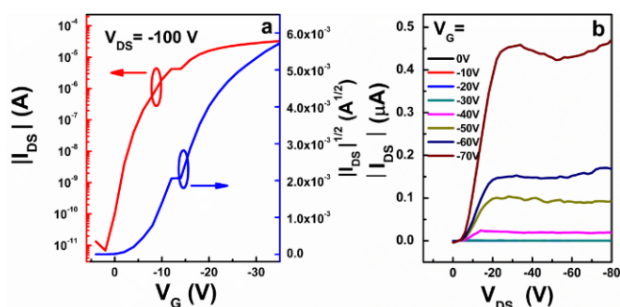


Fig. 3 Transfer (a) and output (b) characteristics of an OFET device based on **6**, spin coated on OTS-treated SiO₂/Si substrate and annealed at 160 °C.

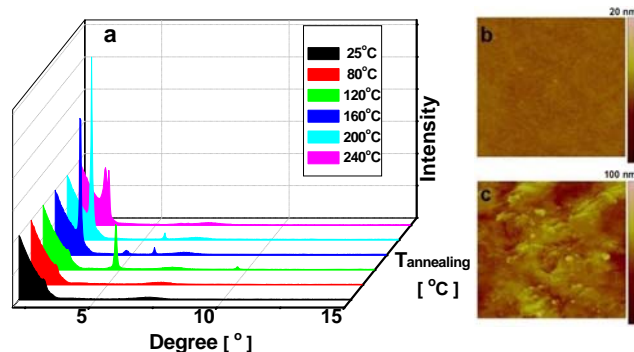


Fig. 4 Temperature variable XRD pattern (a) and AFM images of the thin films of **6** (b: pristine film, c: annealed at 160 °C).

treatment was performed on the gate dielectrics, which were placed in a vacuum oven with OTS at a temperature of 120 °C to form an OTS self-assembled monolayer. Then the thin film were spin-coated on the OTS modified SiO₂/Si substrates from the chloroform solutions (10 mg mL⁻¹) and followed by thermal annealing. The OTFTs characteristics of the devices were all determined at room temperature in air. Representative transfer and output characteristics of the transistors are presented in Fig. 3.

Excitedly, when thermally annealed at 160 °C, thin-film devices exhibited excellent p-type transistor behaviours with high mobility up to 1.13 cm² V⁻¹ s⁻¹ and an on/off ratio of 10⁸. To confirm the results, another batch of seven devices were fabricated, and the average mobility are calculated to be 0.877 cm² V⁻¹ s⁻¹ with a standard deviation (sample) of 0.172. To our best knowledge, the hole mobility is the highest one among pyrene derivatives (Chart S4), close to the hole mobility of highly purified pyrene judged from transient photocurrent and overlap integrals.^{3c} Further raised the annealing temperature to 200 °C resulted in lower mobility of 0.64 cm² V⁻¹ s⁻¹, which was still above 0.5 cm² V⁻¹ s⁻¹. It was also noticed that at the V_G value of -70 V, the output curve decreased rapidly at the V_{DS} values in the range of -30 to -50 V, then increased to the original currency, much apparent in comparison with other output curves at other V_G values. This indicated that the OFET devices might be not so stable, and further improvements should be considered to enhance the stability.

Interestingly, after optimization, the highest electron mobility was only about 10⁻⁵ cm² V⁻¹ s⁻¹ even in inert atmosphere, indicating that the main carriers in **6** are holes. The observed excellent p-type transport behaviour of **6**, which is so far unprecedented for PDIs, should be related to its structural features that influence the molecular packing, possibly leading to the formed “pyrene-channel” in the thin films.¹⁵

To know more about the influence of thermal treatments on the devices performance, thin film morphologies of **6** spin-coated on the OTS modified SiO₂/Si were studied by X-ray diffraction (XRD) and atomic force microscopy (AFM). Fig. 4 and S5 show the AFM topography images of pristine thin films of **6** and thermally treated ones at different temperatures. As shown in Fig. 4b, no obvious crystallinity was found in the as-prepared film. On the contrary, a degree of crystallinity was found in thin film under T_{annealing}=80 °C (Fig. S5b). The AFM images then change dramatically when T_{annealing} increases above 120 °C, and thermal cracks begin to appear over 200 °C, which is an adverse factor for charge transport (Fig. S5c-f). According to XRD patterns (Fig. 4), two groups of peaks, i.e. 4.85° and 9.63°, 2.96° and 5.85° are found under 120 °C and 200 °C, which corresponds to d-spacing of 1.82 nm and 2.98 nm,¹⁶ respectively. Under 160 °C, a combination of two groups appears, suggesting the formation of polymorphism. On the contrast, no peaks appeared under RT and 80 °C. From the viewpoint of relationship between molecular packing and mobility (Table S2), we could draw a conclusion that the d-spacing of 2.98 nm is more favourable to carrier transport, thus the carrier mobility increases with the T_{annealing}. It is also worth noting that the carrier mobility decreases below 200 °C due to the numerous thermal cracks, as mentioned above.

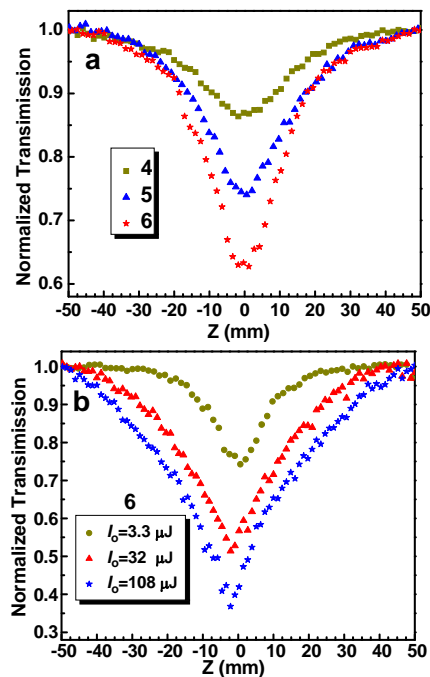


Fig. 5 Open-aperture Z-scan results of **4**, **5** and **6** with the same input fluencies of 10.8 μJ (a) and results of **6** with different input fluencies (b).

Noticed that delocalized π-conjugation systems have been used for optical limiting application,¹⁷ however, no such experimental reports concerned on PDI derivatives. To fully investigate the optoelectronic properties of **6**, we also measured their optical limiting performance. And actually, materials with excellent nonlinear optical (NLO) responses continue to be the focus of theoretical and experimental research due to their potential applications in optical communication, optical data storage, photodynamic therapy and photonic devices.¹⁸ Thus, an open-aperture Z-scan technique was used to measure the NLO absorption coefficient. The results of cyclized products are presented in Fig. 5. The input laser intensity was 10.8 μJ and linear transmittances of all samples were adjusted to

73%. **5** and **6** show an obvious reduction in the transmission on focusing the lens, the minimal normalized transmittance of **6** can reach 63%. As shown in Fig. 5b, better nonlinear optical response emerged when increasing the input intensity. At a lower intensity of 3.3 μJ , the transmittance was 74%, then dropped to be 50% when the intensity increased to 32 μJ , and further decreased to 37% at the intensity of 108 μJ . From the curve shape of open-aperture Z-scan results at 108 μJ , the stability of compound **6** is deduced. And it can be expected that the transmittance will be further decreased when increasing the input intensity. These results show that compound **6** is a good candidate for optical limiting applications.

In summary, three pyrene fused PDI derivatives (**4**, **5** and **6**) were successfully obtained, after conquering the challenge for the control of the structure specificity. The different fused mode of **4** and **5** induces totally different properties, while **6** is a bilaterally extension PDI derivative. Easy fabricated OFET devices based on spin-coated film of **6** exhibit the hole mobility as high as $1.13 \text{ cm}^2 \text{ V}^{-1} \text{ s}^{-1}$ and an on/off ratio of 10^8 in air. Thanks to its special electronic structure, as utilized in optical limiting, **6** also showed excellent performance, and the transmittance can decrease to 37%, when the input laser intensity was 108 μJ . These results, coupled with the good stability, make **6** potential applications in the organic electronic field. Thus, the synthetic method presented in this paper might open up a new way to eliminate the PDI isomers in the cyclization reactions and for the preparation of larger hydrocarbon aromatic rings, perhaps, graphene nanoribbons.

Acknowledgements

We are grateful to the National Science Foundation of China (no. 21325416), and the National Fundamental Key Research Program (2011CB932702) for financial support.

Notes and references

^a Department of Chemistry, Hubei Key Lab on Organic and Polymeric Opto-Electronic Materials, Wuhan University, Wuhan, 430072, China.

E-mail: lizhen@whu.edu.cn or lichemlab@163.com; Fax: +86-27-68756757; Tel: +86-27-68755363.

^b Institute of Chemistry, The Chinese Academy of Sciences, Beijing, China. E-mail: yugui@iccas.ac.cn.

^c Department of Chemistry, Lanzhou University, Lanzhou, China. E-mail: haoli.zhang@lzu.edu.cn.

[†] Electronic supplementary information (ESI) available: Experimental section, ^1H , ^{13}C NMR, MS spectra. See DOI: 10.1039/c000000x/

- 1 (a) S. Demming and H. Langhals, *Chem. Ber.*, 1988, **121**, 225; (b) F. Würthner, *Chem. Commun.*, 2004, **40**, 1564; (c) A. P. H. J. Schennin, J. V. Herrikhuizen, P. Jonkheijm, Z. Chen, F. Würthner, E. W. Meijer, *J. Am. Chem. Soc.*, 2002, **124**, 10252; (d) F. Würthner, Z. Chen, V. Dehm, V. Stepanenko, *Chem. Commun.*, 2006, **42**, 1188; (e) X. Zhang, S. Rehm, M. M. S. Sempere and F. Würthner, *Nat. Chem.*, 2009, **1**, 623.
- 2 (a) Q. Yan, Y. Zhou, Y. Zheng, J. Pei and D. Zhao, *Chem. Sci.*, 2013, **4**, 4389; (b) Z. Yuan, Y. Xiao and X. Qian, *Chem. Commun.*, 2010, **46**, 2772.
- 3 (a) J. E. Anthony, A. Facchetti, M. Heeney, S. R. Marder and X. Zhan, *Adv. Mater.*, 2010, **22**, 3876; (b) C. Wang, H. Dong, W. Hu, Y. Liu and D. Zhu, *Chem. Rev.*, 2012, **112**, 2208; (c) W. Jiang, Y. Li and Z. Wang, *Acc. Chem. Res.*, 2014, **47**, 3135; (d) Y. Lin and X. Zhan, *Mater. Horiz.*, 2014, **1**, 470; (e) J. E. Anthony, A. Facchetti, M. Heeney, S. R. Marder and X. Zhan, *Adv. Mater.*, 2010, **22**, 3876.

- 4 S. Tatemichi, M. Ichikawa, T. Koyama and Y. Taniguchi, *Appl. Phys. Lett.*, 2006, **89**, 112108.
- 5 R. Schmidt, J. H. Oh, Y. S. Sun, M. Derrisch, A. M. Krause, K. Radacki, H. Brauschweig, M. Könemann, P. Erk, Z. Bao and F. Würthner, *J. Am. Chem. Soc.*, 2009, **131**, 6215.
- 6 Y. Zhong, M. T. Trinh, R. Chen, W. wang, P. P. Khlyabich, B. Kumar, Q. Xu, C. Y. Nam, M. Y. Sfeir, C. Black, M. L. Steigerwald, Y. L. Loo, S. Xiao, F. Ng, X. Zhu and C. Nuckolls, *J. Am. Chem. Soc.*, 2014, **136**, 15215.
- 7 (a) H. Langhals and S. Kiener, *J. Org. Chem.*, 2000, **65**, 365; (b) Y. Li, Y. Li, J. Li, C. Li, X. Liu, M. Yuan, H. Liu and S. Wang, *Chem. Eur. J.*, 2006, **12**, 8378; (c) M. Jaggi, C. Blum, B. S. Marti, S. X. Liu, S. Leutwyler and S. Decurtins, *Org. Lett.*, 2010, **12**, 1344; (d) H. Choi, S. Paek, J. Song, C. Kim, N. Cho and J. Ko, *Chem. Commun.*, 2011, **47**, 5509; (e) C. D. Schmidt, N. N. Lang, N. Jux and A. Hirsch, *Chem. Eur. J.*, 2011, **17**, 5289; (f) H. Qian, C. Liu, Z. Wang and D. Zhu, *Chem. Commun.*, 2006, **42**, 4587; (g) W. Yue, A. Lv, J. Gao, W. Jiang, L. Hao, C. Li, Y. Li, L. E. Polander, S. Barlow, W. Hu, S. D. Motta, F. Negri, S. R. Marther and Z. Wang, *J. Am. Chem. Soc.*, 2012, **134**, 5770.
- 8 (a) R. Scholl, C. Seer and R. Weitenböck, *Chem. Ber.*, 1910, **43**, 2202; (b) E. Clar and D. G. Stewart, *J. Am. Chem. Soc.*, 1953, **75**, 2667; (c) C. Jiao, N. Zu, K. Huang, P. Wang and J. Wu, *Org. Lett.*, 2011, **13**, 3652; (d) N. K. S. Davis, A. L. Thompson and H. L. Anderson, *J. Am. Chem. Soc.*, 2011, **133**, 30; (e) Y. Zhong, B. Kumar, S. Oh, M. T. Trinh, Y. Wu, K. Elbert, P. Li, X. Zhu, S. Xiao, F. Ng, M. L. Steigerwald and C. Nuckolls, *J. Am. Chem. Soc.*, 2014, **136**, 8112.
- 9 J. Wu, W. Pisula and K. Müllen, *Chem. Rev.*, 2007, **107**, 718.
- 10 (a) Y. Avlasevich, S. Müller, P. Erk and K. Müllen, *Chem. Eur. J.*, 2007, **13**, 6555; (b) Y. Li, L. Xu, T. Liu, Y. Yu, H. Liu, Y. Li and D. Zhu, *Org. Lett.*, 2011, **13**, 5692.
- 11 (a) T. M. Figueira-Duarte and K. Müllen, *Chem. Rev.*, 2011, **111**, 7260; (b) L. Zöphel, V. Enkelmann, R. Rieger and K. Müllen, *Org. Lett.*, 2011, **13**, 4506.
- 12 (a) D. N. Coventry, A. S. Batsabov, A. E. Goeta, J. A. K. Howard, T. B. Marder and R. N. Perutz, *Chem. Commun.*, 2005, **41**, 2172; (b) Z. Liu, Y. Wang, Y. Chen, J. Liu, Q. Fang, C. Kleeberg and T. B. Marder, *J. Org. Chem.*, 2012, **77**, 7124.
- 13 K. Ota, T. Tanaka and A. Osuka, *Org. Lett.*, 2014, **16**, 2974.
- 14 (a) M. J. Kang, T. Yamamoto, S. Shinamura, E. Miyazaki and K. Takimiya, *Chem. Sci.*, 2010, **1**, 179; (b) J. Mei, Y. Diao, A. L. Appleton, L. Fang and Z. Bao, *J. Am. Chem. Soc.*, 2013, **135**, 6724; (c) S. W. Yun, J. H. Kim, S. Shin, H. Yang, B. K. An, L. Yang and S. Y. Park, *Adv. Mater.*, 2012, **24**, 911; (d) W. Wu, Y. Liu and D. Zhu, *Chem. Soc. Rev.*, 2010, **39**, 1489.
- 15 (a) S. L. Suraru, U. Zschieschang, H. Klauk and F. Würthner, *Chem. Commun.*, 2011, **47**, 11504; (b) R. Lu, Y. Zhou, X. Yan, K. Shi, Y. Zheng, M. Luo, X. Wang, J. Pei, H. Xia, L. Zoppi, K. K. Baldrige, J. S. Siegel and X. Cao, *Chem. Commun.*, 2015, **51**, 1681.
- 16 W. Liu, Y. Zhou, Y. Ma, Y. Cao, J. Wang and J. Pei, *Org. Lett.*, 2007, **8**, 4187.
- 17 (a) H. Liu, J. Xu, Y.-J. Li and Y.-L. Li, *Acc. Chem. Res.*, 2010, **43**, 1496; (b) C. Huang, Y.-L. Li, Y. Song, Y.-J. Li, H. Liu and D. Zhu, *Adv. Mater.*, 2010, **22**, 3532.
- 18 J. L. Brédas, C. Adant, P. tackx, A. Persoons and B. M. Pierce, *Chem. Rev.*, 1994, **94**, 243.